Study of OAM for Communication and Radar

Daniel Orfeo
Department of Mechanical Engineering
Univeristy of Vermont
Burlington, USA
dan.orfeo@protonmail.com

Dryver Huston
Department of Mechanical Engineering
University of Vermont
Burlington, USA
dryver.huston@uvm.edu

Tian Xia
Department of Electrical and Biomedical Engineering
University of Vermont
Burlington, USA
txia@uvm.edu

2021 IEEE Radar Conference (RadarConf21) | 978-1-7281-7609-3/20/$31.00 ©2021 IEEE | DOI: 10.1109/RadarConf2147009.2021.9455299

***Abstract*—Radio-frequency sensing and communication systems which use a waveform for more than one function offer the promise of improved spectral efficiency and streamlined hardware requirements. Control of orbital angular momentum (OAM) may be used to increase data-rates and improve radar sensitivity to certain chiral targets. This paper presents finite-difference time-domain simulations which model a gigahertz-frequency OAM radar capable of transmitting information via OAM-mode modulation. The unique chirality-detection capability of OAM radar is demonstrated, as well as simple information transmission. Simulation scope and radar specifications are designed with an eye toward developing a dual function ground penetrating radar (GPR) with OAM mode control.**

Keywords—radar, communication, microwave, OAM, GPR

I. INTRODUCTION

Spectral efficiency has become a major concern for the design of next-generation radio frequency (RF) systems. At the same time, computational power and hardware capabilities have increased, opening the door for systems which can perform multiple functions with the same waveform. Possible applications include a vehicle-to-vehicle communication system that can also warn of impending collisions [1], or a ground penetrating radar (GPR) system[2][3] that can self-localize via a communication timing network. This type of dual function waveform could also save money by eliminating the redundant hardware that is present when employing multiple single-function systems.

Control of orbital angular momentum (OAM) is an innovative technique which facilitates use of an added degree of freedom to improve waveform capabilities. Unlike spin angular momentum (SAM) which corresponds to electromagnetic polarization, OAM is dependent on a field's spatial phase distribution[4]. For this reason, waveforms with nonzero OAM are said to be spatially *structured*. This structure takes the form of a helix, with an optical vortex at the center of the intensity profile [5]. There are different integer-number OAM modes which are found to be mathematically orthogonal. Mode n corresponds to an n-helix, and the sign of the mode indicates helix direction, defined as positive (left-handed), or negative (right-handed). Note that OAM is distinct from circular polarization: waveforms with nonzero OAM are not plane waves.

OAM is of significant interest in the development of new RF systems due to its property of modal orthogonality. It may be possible to multiplex information on different OAM modes, thereby increasing data-rates or improving spectral efficiency [6]. OAM also shows promise as a novel waveform for certain radar applications. Just as antenna configurations [7] and polarization can be manipulated to improve signal returns for hard-to-detect targets, OAM may be useful for its ability to detect chirality and improve the detection of targets with chiral properties [8]. A chiral object is asymmetric such that it is not superimposable with its mirror image, for example, a left or right-handed spiral staircase. Applications include the detection of propellers [9], including the props used by quadcopter UAVs. OAM can also be used to measure the rotational doppler shift of a target [10].

This paper presents a scheme for unifying these concepts with a dual function OAM waveform. The resultant sensing and communication system exploits the unique scattering properties of microwaves with nonzero OAM. The scheme is evaluated using a series of finite-difference time-domain simulations conducted with the program gprMax [11]. A goal of this inquiry is to adapt these findings for GPR usage. Intersecting underground utility pipes can have chiral spatial properties. It is of interest if compared to a traditional plane wave GPR pulse, OAM GPR may provide advantages for identifying buried targets in congested or overlapping configurations. Because of this, the dimensions and frequencies in this paper are chosen for compatibility with GPR applications. Over long distances, an OAM beam may undergo a significant amount of divergence [12], which necessitates a very large receiver array to measure the complete OAM field. An upshot of designing for a GPR application is that over short distances on the order of one to ten meters a microwave OAM beam undergoes only a small amount of divergence, eliminating the need for an oversized receiver array.

This work has been supported by Defense University Research Instrumentation Program (DURIP) U.S. Army contract no. W911NF1810193, U.S. Army contract W909MY-17-C-0020 with White River Technologies, Inc., U.S. National Science Foundation grants 1647095 and 1640687, University of Vermont SPARK Fund, UVM Office for the Vice President for Research, and the Vermont Space Grant Consortium under NASA Cooperative Agreement NNX15AP86H.

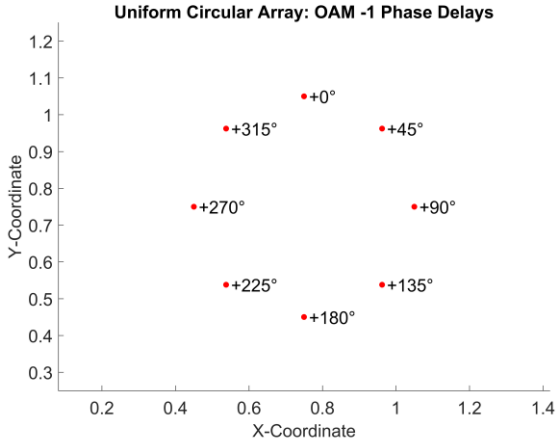

Fig. 1 Phase delays to generate an OAM -1 (right-handed) waveform with a uniform circular antenna array. Coordinate distances are shown in meters, antenna locations are indicated by red dots. In this view the waveform is propagating out of the page, directly toward the reader.

II. Methodology

A. System Overview

The system overview is as follows. An encoder maps different binary bits to different OAM modes via the OAM shift keying (OAM-SK) method. A uniform circular array (UCA) transceiver broadcasts microwaves pulses encoded with this information to a UCA receiver, where the message is decoded. If this transmission is interrupted by a transient target, the signal reflects back to the transceiver UCA, at which point information about the target can be interpreted due to the unique properties of OAM waveforms.

B. Generation of Microwaves with OAM

Microwaves with OAM can be produced by a UCA with azimuthally dependent phase delays programmed for each sine-wave emitter [13]. This sc heme, shown in Fig. 1, creates the helix-shap ed spatially dependent phase distribution. Phase delays are implemented by loading an appropriately phase-shifted sine wave into each channel. For a UCA of N antennas, the signal y for the n^{th} antenna in the array with phase delay $\varphi = {}^{2\pi}/_{N}$ is defined:

$$y(n) = A * \sin(2\pi f t + (n-1) * \varphi) \qquad (1)$$

where A is amplitude, f is frequency, and t is the time vector defined by a constant predefined time step. In the case of the right-handed OAM -1 waveform in Fig. 1, the phase-delay angle matches the azimuth angle exactly. Higher-order OAM modes have more complex geometries—for example, in the case of an OAM -2 waveform, 180-degrees of azimuth corresponds to 360-degrees of phase delay.

The axis coordinates in Fig. 1 are based on the coordinate system used in the following simulation experiments. The array is designed with a 0.3-meter radius, which is equivalent to one-wavelength of the 1-GHz sine waves utilized. 1-GHz signals are within the frequency range typically utilized by GPR, and the 0.6-meter array is comparably sized to available pushcart GPR systems [14].

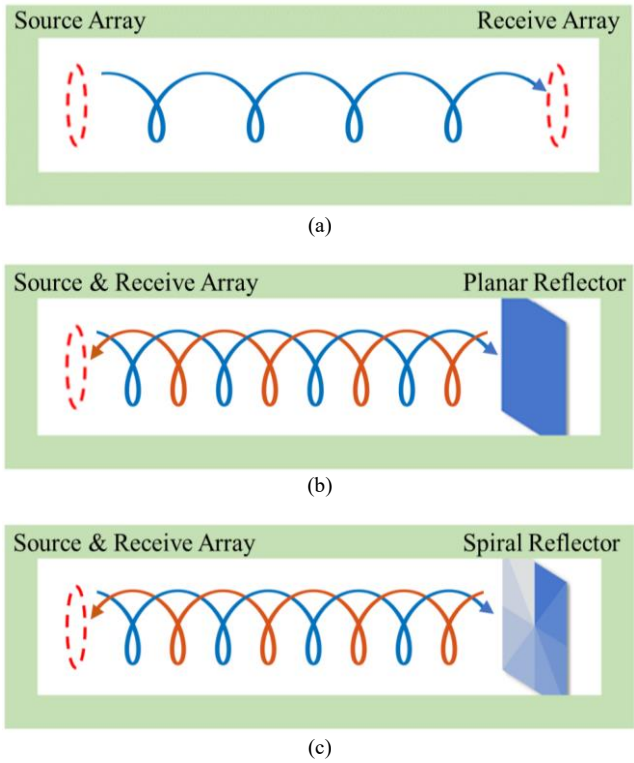

Fig. 2 Geometry views for three OAM sensing and communication simulations using the FDTD method. (a) An 8-element transmitter array (dashed circle on left) broadcasts a binary signal to an 8-element receiver array via the OAM-SK encoding method. (b) An 8-element transceiver array (left) reflects an OAM-SK message off a planar target and recovers chirality and range information about the target. (c) The same 8-element transceiver array reflects an OAM-SK message off a stepped spiral target.

C. FDTD Simulation in gprMax

The radar and communication system demonstrated in this paper was simulated in the program gprMax using the finite-difference time-domain (FDTD) technique, also called Yee's method. Maxwell's equations are discretized in space, allowing calculation of the electric field for each point at progressing time instants. Simulation geometries are shown in Fig. 2. Fig. 2(a) shows an 8-element transmitter array that broadcasts to an 8-element receiver array via the OAM-SK method [15], in which information is encoded by the OAM mode number. In Fig. 2(b) and Fig. 2(c) an 8-element transceiver array transmits an OAM-SK message which reflects off a target. Although the presence of the target may prevent the message from reaching a freestanding receiver array, analysis of the reflected OAM-SK signal (received by the transceiver array) enables target ranging and detection of target chirality. The case of a planar target is shown in Fig. 2(b) and a spiral target [16] is shown in Fig. 2(c). In this manner, the simulations demonstrate independent communication and radar functionality for the proposed OAM system. One can imagine a real-world scenario in which an A to B communication link is intersected by a passing target. This causes a reflection back to the source at transceiver A, where ranging and chirality information are extracted.

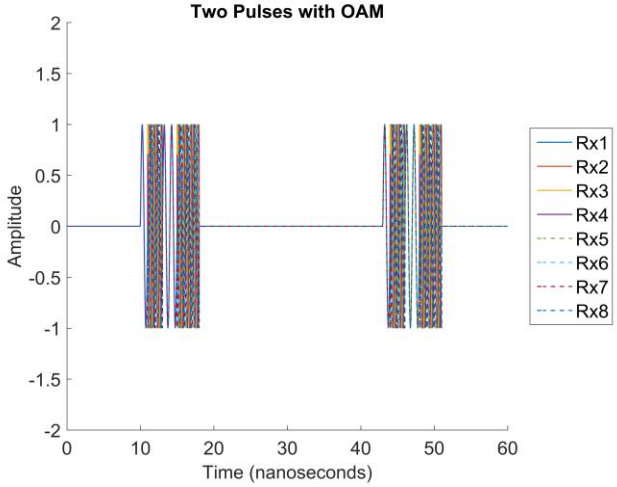

Fig. 3 Two pulses with programmed OAM characteristics. For the sake of illustration in this example, the pulse repetition interval T is 25 nanoseconds and the pulse width τ is 8 nanoseconds. Practically, T may be much larger, up to the order of 1 millisecond.

The simulation domain is 1.5-meters square by 4.75-meters long, including a quarter-meter thick Perfectly Matched Layer (PML) absorbing boundary condition on the inside of each face (light green in Fig. 2). Targets are 3.5-meters from the transceiver array and fill the entire cross-section of the domain space. The time step is 7.7-picoseconds and each simulation is 59 nanoseconds in duration. Spatial resolution in the X, Y, and Z directions is 4 millimeters. Antenna array elements have the coordinates specified in Fig. 1.

D. Radar Pulses with OAM

The OAM-SK signal is encoded inside a radar pulse structure as shown in Fig. 3. The pulse structure allows the radar to perform timing for target ranging. Each pulse contains a user-programmed number of 8-bit bytes. In this case, each pulse contains a single byte, 01100111, which translates to the English character "g". Each pulse can be programmed to contain unique information, as desired. The data rate is proportional to the number of bytes in a pulse, as well as the pulse repetition frequency. OAM modes are identified by time-gating the received data and measuring the relative phases of the signals received at each antenna in the receiver array.

III. Results

A. A-to-B Transmission

Fig. 4(a) shows the results obtained using the A-to-B transmission geometry shown in Fig. 2(a). For visual clarity, the plot is cropped to highlight a single OAM pulse. A data link is formed when signals are transmitted from the array on the left side of the geometry of Fig. 2(a) and received by the array at the right side of Fig. 2(a).

OAM-SK is used to encode the message "go" in 8-bit binary. OAM mode 0 corresponds to a zero-bit, and OAM mode -1 corresponds to a 1-bit. By time-gating the received waveform (vertical black lines in Fig. 4(a)), the mode-bits can be identified: OAM mode 0 waveforms are in-phase, while OAM mode -1

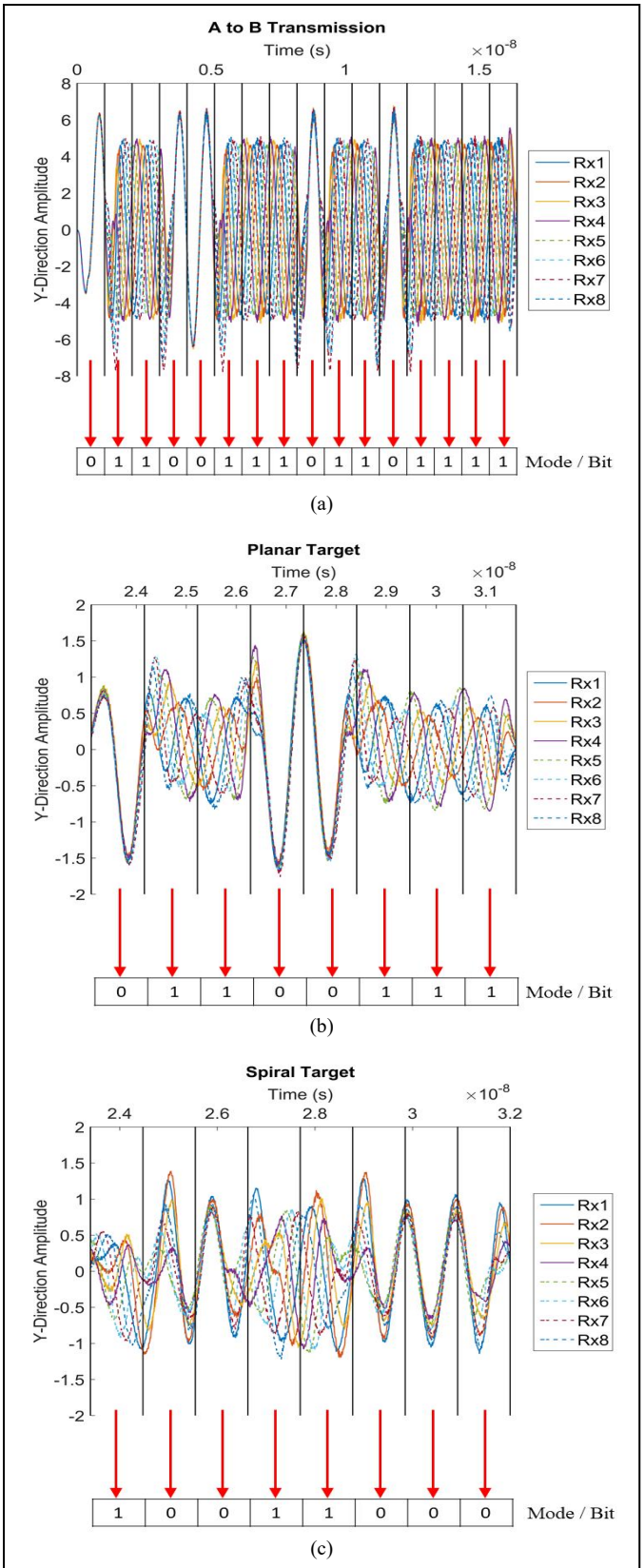

Fig. 4 Received data in OAM pulses for (a) A-to-B communication, (b) signal reflection from planar target, and (c) signal reflection from chiral target. OAM-SK encodes binary information where mode 0 is "0" and mode -1 is "1".

waveforms are out-of-phase, per the phase delays defined in Fig. 1. (An OAM -1 waveform is received in the order Rx8, Rx7, Rx6, Rx5, Rx4, Rx3, Rx2, Rx1.) In this way, binary code is extracted from the OAM-SK signal: 0110011101101111. Translating recovers the message: "go". This demonstrates an A-to-B data link using the OAM-SK method. The following sections consider what happens when this link is interrupted by a transient target.

B. Planar Target

In Fig. 2(b) the A-to-B link is interrupted by a planar target perpendicular to the signal. As before, 8-bit data are encoded via OAM-SK where OAM mode 0 corresponds to a zero-bit and OAM mode -1 corresponds to a 1-bit. The signal is broadcast from the array on the left side of the geometry view in Fig. 2(b). It then reflects off the planar target (right side) back toward the first array, where it is received and digitized.

Fig. 4(b) shows the reflected data received by the transceiver array. In-phase (mode 0) and phased (mode -1) sections are identified and binary bits are extracted: 01100111. Translating recovers the single-character message: "g". A chiral target would alter the OAM modes used in the OAM-SK encoding, and alter the message. Because the OAM modes are unmodified compared to the transmitted signal (i.e., the signal received in the A to B transmission simulation) and the message is preserved, it is concluded that the target does not have chiral properties, and is planar. This simulation demonstrates the ability of an OAM-SK data link to provide radar functionality and identify the chirality of a transient target.

C. Spiral Target

The simulation illustrated in Fig. 2(c) is identical to the test in Fig. 2(b) and Fig. 4(b) except a spiral target is used in place of the planar target. This change is made to demonstrate the ability of the OAM-SK data link to discriminate and identify objects with planar or chiral properties. The chiral target on the right side of Fig. 2(c) is a spiral-wedge design composed of eight triangular sections [6, 14]. From top-center, these sections have progressively decreasing thickness when measured in the clockwise direction. The total change in thickness is 15-cm, equivalent to one-half wavelength of the 1-GHz signal used in the experiment. Because different positions on the transceiver azimuth have different round-trip path lengths from transceiver to target back to the transceiver, this right-handed target has the ability to "add" OAM to an incident signal. This means that an incident plane wave (OAM 0) will be shifted to OAM +1 as it reflects, and an incident OAM -1 waveform will be shifted to OAM 0 as it reflects.

Fig. 4(c) shows the received signal after it reflects off the spiral target. The first, fourth, and fifth time-gated sections display a phased signal order Rx1, Rx2, Rx3, Rx4, Rx5, Rx6, Rx7, Rx8, indicative of OAM +1. The remaining sections are in-phase, indicating OAM 0. Compared to the planar reflector case in Fig. 4(b), each time-gated bit in Fig. 4(c) has had its OAM mode increased by one. This indicates that the reflective target interrupting the OAM-SK data link has right-handed chiral properties. Translating mode 0 to a 0-bit and mode 1 to a 1-bit, the following binary code is recovered: 10011000. This is opposite the known transmitted signal (01100111), further indicating target chirality.

Of course, in addition to communication and target chirality detection, the radar and communication OAM-SK link can also provide target ranging by timing the OAM pulses. The X-axis time stamps in Fig. 4(b) and Fig. 4(c) indicate a round-trip signal path time of approximately 23.4 nanoseconds. At the speed of light, this indicates the target is 3.5 meters from the transceiver array, which is precisely the value specified in the simulation geometry.

IV. Discussion

This paper presents a successful simulation proof-of-concept for a communication and radar system which exploits OAM for both data transmission and sensing purposes. Binary information is transmitted on an A-to-B data link via OAM-SK modulation while OAM scattering provides information on the chirality and range of transient objects that pass-through the link. Crucially, because OAM modes are orthogonal and independent of polarization, this scheme could be implemented as a single layer of a more sophisticated multiplexed system.

The spiral target used in this study is engineered to precisely increase by one the OAM mode of an incident signal. This design decision was made to clearly illustrate the potential of this radar-communication concept. Future work will need to explicitly consider the effects of arbitrary and irregular chiral objects. An irregular target could lead to an imperfect OAM phase shift or a superposition of multiple OAM modes. In this case, a more sophisticated method to identify OAM modal content could be employed, where OAM modes are identified via a modal-spectral analysis similar to Fourier transformation [13, 17, 18].

In this investigation, the system geometry and test targets were chosen to facilitate a simple transition to laboratory testing. Future work will focus on laboratory validation, dynamic target movement, as well as an examination of multipath effects and partial target illumination.

References

[1] A. Hassanien, M. G. Amin, E. Aboutanios, and B. Himed, "Dual-Function Radar Communication Systems: A Solution to the Spectrum Congestion Problem," *IEEE Signal Processing Magazine,* vol. 36, no. 5, pp. 115-126, 2019.

[2] Huston, D., Xia, T., Zhang, Y., Fan, T., Orfeo, D. and Razinger, J., 2017, April. Urban underground infrastructure mapping and assessment. In *Sensors and Smart Structures Technologies for Civil, Mechanical, and Aerospace Systems 2017* (Vol. 10168, p. 101680M). International Society for Optics and Photonics.

[3] Jiao L, Ye Q, Cao X, Huston D, Xia T. Identifying concrete structure defects in GPR image. Measurement. 2020 Aug 1;160:107839.

[4] L. Allen, M. Beijersbergen, R. Spreeuw, and J. Woerdman, "Orbital angular momentum of light and

transformation of Laguerre Gaussian Laser modes," *Physical review. A,* vol. 45, pp. 8185-8189, 07/01 1992.

[5] T. Yuan, H. Wang, Y. Cheng, and Y. Qin, "Electromagnetic Vortex-Based Radar Imaging Using a Single Receiving Antenna: Theory and Experimental Results," *Sensors,* vol. 17, no. 3, Mar 19 2017.

[6] L. Cheng, W. Hong, and Z.-C. Hao, "Generation of electromagnetic waves with arbitrary orbital angular momentum modes," *Scientific reports*, vol. 4, p. 4814Accessed on: 2014. doi: 10.1038/srep04814 Available: https://www.ncbi.nlm.nih.gov/pmc/articles/pmid/24770669/pdf/?tool=EBI

[7] D. Orfeo, Y. Zhang, D. Burns, J. S. Miller, D. R. Huston, and T. Xia, "Bistatic antenna configurations for air-launched ground penetrating radar," *Journal of Applied Remote Sensing,* vol. 13, no. 2, pp. 1-9, 9, 2019.

[8] D. Orfeo, D. Burns, D. Huston, and T. Xia, "Electrically controlled phased array OAM radar," in *SPIE Defense + Commercial Sensing Radar Sensor Technology XXIV*, Anaheim, California United States, 2020: SPIE.

[9] B. Liu, H. Chu, H. Giddens, R. Li, and Y. Hao, "Experimental Observation of Linear and Rotational Doppler Shifts from Several Designer Surfaces," *Scientific Reports,* vol. 9, no. 1, p. 8971, 2019/06/20 2019.

[10] G. M. Gibson, E. Toninelli, S. A. R. Horsley, G. C. Spalding, E. Hendry, D. B. Phillips, and M. J. Padgett, "Reversal of orbital angular momentum arising from an extreme Doppler shift," (in eng), *Proceedings of the National Academy of Sciences of the United States of America,* vol. 115, no. 15, pp. 3800-3803, 2018.

[11] C. Warren, A. Giannopoulos, and I. Giannakis, "gprMax: Open source software to simulate electromagnetic wave propagation for Ground Penetrating Radar," *Computer Physics Communications,* vol. 209, pp. 163-170, 2016/12/01/ 2016.

[12] M. J. Padgett, F. M. Miatto, M. P. J. Lavery, A. Zeilinger, and R. W. Boyd, "Divergence of an orbital-angular-momentum-carrying beam upon propagation," *New Journal of Physics,* vol. 17, no. 2, p. 023011, 2015/02/04 2015.

[13] B. Thidé, H. Then, J. Sjöholm, K. Palmer, J. Bergman, T. D. Carozzi, Y. N. Istomin, N. H. Ibragimov, and R. Khamitova, "Utilization of Photon Orbital Angular Momentum in the Low-Frequency Radio Domain," *Physical Review Letters,* vol. 99, no. 8, p. 087701, 08/22/ 2007.

[14] GSSI. (2017). *BridgeScan GPR Bridge Inspection Equipment*. Available: https://www.geophysical.com/products/bridgescan

[15] R. Chen, H. Zhou, M. Moretti, X. Wang, and J. Li, "Orbital Angular Momentum Waves: Generation, Detection, and Emerging Applications," *IEEE Communications Surveys & Tutorials,* vol. 22, no. 2, pp. 840-868, 2020.

[16] F. Tamburini, E. Mari, B. Thidé, C. Barbieri, and F. Romanato, "Experimental verification of photon angular momentum and vorticity with radio techniques," *Applied Physics Letters,* vol. 99, no. 20, p. 204102, 2011/11/14 2011.

[17] H. Wu, Y. Yuan, Z. Zhang, and J. Cang, "UCA-based orbital angular momentum radio beam generation and reception under different array configurations," 12/18 2014.

[18] S. Fu, Y. Zhai, J. Zhang, X. Liu, R. Song, H. Zhou, and C. Gao, "Universal orbital angular momentum spectrum analyzer for beams," *PhotoniX,* vol. 1, no. 1, p. 19, 2020/08/17 2020.